Nonthermal particle acceleration from maximum entropy in collisionless plasmas

Vladimir Zhdankin[1]†

[1]Center for Computational Astrophysics, Flatiron Institute, 162 Fifth Avenue, New York, NY 10010, USA

(Received xx; revised xx; accepted xx)

Dissipative processes cause collisionless plasmas in many systems to develop nonthermal particle distributions with broad power-law tails. The prevalence of power-law energy distributions in space/astrophysical observations and kinetic simulations of systems with a variety of acceleration and trapping (or escape) mechanisms poses a deep mystery. We consider the possibility that such distributions can be modeled from maximum-entropy principles, when accounting for generalizations beyond the Boltzmann-Gibbs entropy. Using a dimensional representation of entropy (related to the Renyi and Tsallis entropies), we derive generalized maximum-entropy distributions with a power-law tail determined by the energy scale at which irreversible dissipation occurs. By assuming that particles are energized by an amount comparable to the free energy (per particle) before equilibrating, we derive a formula for the power-law index as a function of plasma parameters for magnetic dissipation in systems with sufficiently complex topologies. The model reproduces several results from kinetic simulations of relativistic turbulence and magnetic reconnection.

1. Introduction

Nonthermal energetic particles are ubiquitous in collisionless plasmas, being observed in laboratory experiments, planetary magnetospheres (Birn *et al.* 2012), the solar wind (Fisk & Gloeckler 2007), the solar corona (Aschwanden 2002), and high-energy astrophysical systems. It was long recognized that nonthermal particles are a generic consequence of collisionless plasma physics, as the absence of Coulomb collisions precludes relaxation to a thermal equilibrium (e.g., Fermi 1949, 1954; Parker & Tidman 1958). More recently, first-principles numerical simulations demonstrated efficient particle acceleration from shocks (Spitkovsky 2008; Sironi & Spitkovsky 2010; Caprioli & Spitkovsky 2014), magnetic reconnection (Sironi & Spitkovsky 2014; Guo *et al.* 2014; Werner *et al.* 2016; Li *et al.* 2019), relativistic turbulence (Zhdankin *et al.* 2017; Comisso & Sironi 2018), and various instabilities (e.g., Hoshino 2013; Kunz *et al.* 2016; Nalewajko *et al.* 2016; Alves *et al.* 2018; Ley *et al.* 2019; Sironi *et al.* 2021). In observations and simulations, particle energy distributions frequently exhibit power-law tails in which the index α can range from hard ($\alpha \sim 1$) to soft ($\alpha \gg 1$) values, depending on system parameters. Determining why power-law distributions form and predicting α as a function of parameters are topics of fundamental importance.

This Letter explores the possibility that power-law distributions in collisionless plasmas can be explained by maximum-entropy principles, when considering nonextensive entropy measures beyond the traditional Boltzmann-Gibbs (BG) entropy. There is no *a priori* reason for a collisionless plasma to relax to a state of maximum BG entropy. Given that

† Email address for correspondence: vzhdankin@flatironinstitute.org

plasma dissipation processes are macroscopically irreversible, the question is then, what type of entropy (if any) does a collisionless plasma maximize upon equilibration?

A framework for quantifying generalized entropy based on dimensional representations of entropy derived from the Casimir invariants of the Vlasov equation was recently developed in Zhdankin (2021). This framework shares similarities to the nonextensive entropies of Renyi (Rényi 1961) and Tsallis (Tsallis 1988), but enables a connection with irreversible processes occurring at various energy scales within the plasma. Using this framework, we derive a generalized maximum-entropy (GME) distribution (equivalent to the Tsallis distribution) that has a power-law tail at high energies, resembling numerical and observational results in the literature. For a given number of particles and kinetic energy content, there is only one unconstrained free parameter (linked to α), determined by the energy scale at which entropy is maximized.

After deriving the GME distribution, we propose a model for determining the power-law index α as a function of physical parameters, for systems governed by magnetic dissipation with sufficiently complex topologies. By assuming that particles are energized by an amount comparable to the free energy per particle before equilibrating, we derive an equation for α versus plasma beta and fluctuation amplitude, indicating that nonthermal particle acceleration is efficient when β is low and fluctuations are strong. We compare the model predictions to numerical results from the literature on relativistic turbulence and magnetic reconnection, showing that the model is able to reproduce some observed trends such as the scaling of α with the magnetization σ. The GME model also provides a resolution for why power-law distributions are often similar for distinct processes (with diverse escape/trapping mechanisms) and for varying spatial dimensionality (2D versus 3D).

The GME framework provides a route to understanding particle acceleration that is distinct from standard approaches based on quasilinear theory and its extensions. The limitations and applicability of the model are further discussed in the conclusions.

2. Model for generalized maximum-entropy distribution

Consider a collisionless plasma in a closed system. The evolution of the fine-grained particle distribution for a given species can be represented by the (relativistic) Vlasov equation,

$$\partial_t f + \boldsymbol{v} \cdot \nabla f + \boldsymbol{F} \cdot \partial_{\boldsymbol{p}} f = 0\,, \tag{2.1}$$

where $f(\boldsymbol{x}, \boldsymbol{p}, t)$ is the particle momentum distribution function (normalized such that $\int d^3p d^3x f = N$ is the total number of particles), $\boldsymbol{v} = \boldsymbol{p}c/(m^2c^2 + p^2)^{1/2}$ is the particle velocity (with m the particle mass), and $\boldsymbol{F}(\boldsymbol{x}, \boldsymbol{p}, t)$ is a phase-space conserving force field ($\partial_{\boldsymbol{p}} \cdot \boldsymbol{F} = 0$), containing the electromagnetic force and external forces. Eq. 2.1 can be applied to any particle species, with appropriate $\boldsymbol{F}$. We denote particle kinetic energy by $E(p) = (m^2c^4 + p^2c^2)^{1/2} - mc^2$ and the system-averaged kinetic energy by $\overline{E}$.

The Vlasov equation formally conserves the BG entropy $S = -\int d^3x d^3p f \log f$ as well as an infinite set of quantities known as the Casimir invariants. The latter can be manipulated to yield quantities with dimensions of momentum, introduced in Ref. (Zhdankin 2021) as the *Casimir momenta*:

$$p_{c,\chi}(f) \equiv n_0^{1/3} \left(\frac{1}{N} \int d^3x d^3p f^\chi \right)^{-1/3(\chi-1)}\,, \tag{2.2}$$

where n_0 is the mean particle number density and $\chi > 0$ is a free index that parameterizes the weight toward different regions of phase space: large (small) values of χ

are sensitive to low (high) energies. The phase-space integral in Eq. 2.2 resembles those used in the nonextensive entropies of Renyi (Rényi 1961) and Tsallis (Tsallis 1988). The Casimir momenta, however, manipulate this integral into a dimensional form that is interpretable physically. In particular, the anomalous growth of $p_{c,\chi}$ is indicative of irreversible entropy production at the corresponding momentum scale in phase space (with $\chi \to 0$ corresponding to momenta far in the tail, and $\chi \to \infty$ corresponding to momenta near the mode).

As described in Zhdankin (2021), $p_{c,\chi}$ share many properties with the BG entropy S: 1) they reduce to a dimensionalized version of the BG entropy when $\chi \to 1$, as $p_{c,\chi\to 1} = n_0^{1/3} e^{S/3N}$; 2) they are maximized when f is isotropic and uniform; and 3) while ideally conserved by the Vlasov equation, the formation of fine-scale structure breaks conservation of $p_{c,\chi}$ for f measured at coarse-grained scales. Zhdankin (2021) also argued that $p_{c,\chi}$ associated with coarse-grained f will tend to increase (irreversibly) when energy is injected into the system, for generic complex processes; this was demonstrated by 2D kinetic simulations of relativistic turbulence. Phenomena such as the entropy cascade may lead to anomalous entropy production through finite collisionality (Schekochihin *et al.* 2009; Eyink 2018).

The infinite number of generalized entropies represented by $p_{c,\chi}$ complicates the application of a maximum entropy principle. Only when dissipation occurs collisionally or at small enough energy scales ($\chi \sim 1$) is the BG entropy maximized. In general, mechanisms of anomalous entropy production can operate over a spectrum of scales, so a scale-by-scale understanding of the plasma physical processes is necessary to model the system.

In this Letter, we consider the idealized situation where entropy is maximized at a single energy scale, represented by p_{c,χ_d} with a given index χ_d where the subscript d denotes “dissipation”. Suppose that the system evolves to maximize p_{c,χ_d}. The GME distribution is uniform and isotropic $f(\boldsymbol{p}, \boldsymbol{x}) = f(p)$, and can be derived from the functional

$$\mathcal{L} = N^{1/3} \left(\int d^3p f^{\chi_d}/N \right)^{-1/3(\chi_d - 1)} - \lambda_1 \left(\int d^3p f - N \right) - \lambda_2 \left[\int d^3p E(p) f - N\overline{E} \right] ,$$

where λ_i are Lagrange multipliers enforcing number and energy constraints. By requiring $\delta\mathcal{L} = 0$ upon variations of the distribution δf, we obtain

$$\frac{p_{c,\chi_d}^{3\chi_d - 2} \chi_d f^{\chi_d - 1}}{3(1-\chi_d) N^{2/3}} - \lambda_1 - \lambda_2 E(p) = 0 \tag{2.3}$$

which leads to the GME distribution

$$f = C \left[E(p)/E_b + 1 \right]^{-1/(1-\chi_d)} , \tag{2.4}$$

where C and E_b are the normalization factor and characteristic energy, determined by requiring $4\pi \int dp p^2 f = N$ and $4\pi \int dp p^2 E(p) f = N\overline{E}$. Note that Eq. 2.4 is operationally equivalent to the Tsallis distribution (Tsallis 1988). We will restrict our attention to $\chi_d < 1$, in which case there is a power-law tail (whereas $\chi_d > 1$ would lead to a narrow distribution with sharp cutoff). The derivation of Eq. 2.4 from maximizing a dimensional representation of generalized entropy is the first main result of this work.

In the ultra-relativistic (UR) limit, $\overline{E} \gg mc^2$, the GME distribution (Eq. 2.4) becomes

$$f \xrightarrow{\mathrm{UR}} C(p/p_b + 1)^{-\alpha - 2} \tag{2.5}$$

where $\alpha = (2\chi_d - 1)/(1 - \chi_d)$, $C = N(\alpha - 1)\alpha(\alpha + 1)/8\pi p_b^3$, and $p_b = (\alpha - 2)\overline{E}/3c$. In the non-relativistic (NR) limit, $\overline{E} \ll mc^2$, Eq. 2.4 becomes

$$f \xrightarrow{\rm NR} C \left(p^2/p_b^2 + 1\right)^{-\alpha-1/2} \tag{2.6}$$

where $\alpha = (1+\chi_d)/2(1-\chi_d)$, $C = N\Gamma(\alpha+1/2)/\pi^{3/2}p_b^3\Gamma(\alpha-1)$, and $p_b = [4(\alpha-2)m\overline{E}/3]^{1/2}$. The NR expression (Eq. 2.6) is equivalent to the kappa distribution that is widely used to model nonthermal distributions in space plasmas (e.g., Pierrard & Lazar 2010; Livadiotis & McComas 2013) and was previously shown to arise from Tsallis statistics (Milovanov & Zelenyi 2000; Leubner 2002; Livadiotis & McComas 2009).

In both limits, we used α to denote the power-law index of the corresponding energy distribution,

$$F(E) = \frac{dp}{dE} 4\pi p^2 f(p)|_{p=[E(E+2mc^2)]^{1/2}/c}\,, \tag{2.7}$$

such that $F(E) \propto E^{-\alpha}$ at high energies. Since the GME distribution has an infinite extent in energy, $\alpha > 2$ is necessary for finite $\overline{E}$. Thus, the domain is $3/4 < \chi_d < 1$ for the UR case and $3/5 < \chi_d < 1$ for the NR case. Also note that $\chi_d \to 1$ ($\alpha \to \infty$) recovers the thermal (Maxwell-Jüttner) distribution, using the identity $(A/x+1)^{-x} = e^{-A}$ as $x \to \infty$ for any A.

3. Model for power-law index

Suppose that the dynamics are sufficiently complex to cause the initial distribution (which is arbitrary) to evolve into the GME state. For this state to be maintained with a constant index α in an evolving system, $p_{c,\chi}$ for all χ must grow in proportion with the mean momentum, preserving their relative hierarchy. One can then compare the momentum at which entropy is maximized, p_{c,χ_d}, with the momentum of the typical particle given by $p_{c,\infty}$ (note that $p_{c,\infty}$ lies close to p_b). Evaluating $p_{c,\chi_d}/p_{c,\infty}$ using Eq. 2.2 with the GME distribution (Eq. 2.4), one obtains in the UR limit:

$$\frac{p_{c,\chi_d}}{p_{c,\infty}} \xrightarrow{\rm UR} \left(\frac{\alpha+1}{\alpha-2}\right)^{(\alpha+2)/3}\,, \tag{3.1}$$

and in the NR limit:

$$\frac{p_{c,\chi_d}}{p_{c,\infty}} \xrightarrow{\rm NR} \left(\frac{\alpha-1/2}{\alpha-2}\right)^{(2\alpha+1)/6}\,. \tag{3.2}$$

This relates the power-law index α to the maximum-entropy scale, which can be modeled phenomenologically (as considered below). In Fig. 1, we show α versus $p_{c,\chi_d}/p_{c,\infty}$, separately for the UR (Eq. 3.1) and NR (Eq. 3.2) limits. Note the divergence $\alpha \to \infty$ when $p_{c,\chi_d}/p_{c,\infty} \to e \approx 2.72$ (UR case) or $p_{c,\chi_d}/p_{c,\infty} \to e^{1/2} \approx 1.65$ (NR case). Thus, if entropy is maximized at momentum scales sufficiently close to the peak of the distribution, then a thermal distribution is recovered (similar to a collisional plasma). When $p_{c,\chi_d}/p_{c,\infty}$ becomes larger than a factor of few, the nonthermal state is obtained, with $\alpha \to 2$ for $p_{c,\chi_d}/p_{c,\infty} \gg 1$. Thus, in both the UR and the NR limit, *the distribution will relax to the nonthermal state if entropy is maximized at momenta scales in the tail of the distribution.*

Physical considerations are necessary to determine $p_{c,\chi_d}/p_{c,\infty}$ as a function of system parameters, from which one can extract α. In general, this will need to be informed by numerical simulations and analytical considerations for the given process.

For this Letter, we consider a simplified scenario to estimate the momentum scale of maximum entropy that arises from the dissipation of magnetic energy in complex field topologies (via magnetic reconnection, turbulence, or instabilities). We suppose

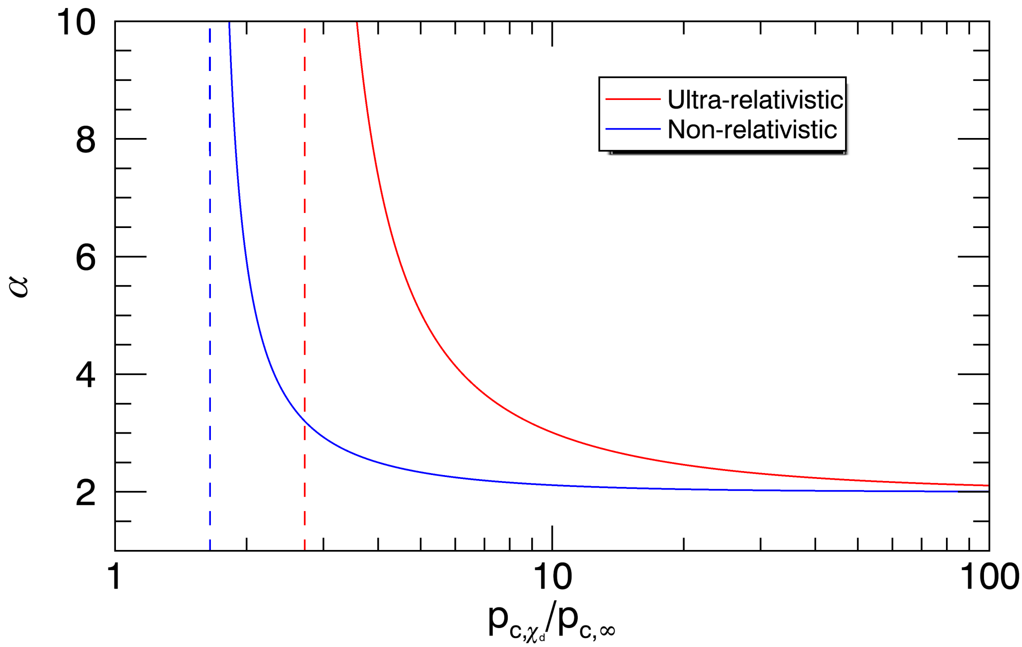

FIGURE 1. The energy power-law index α of the GME distribution versus the ratio between the entropy-maximizing momentum p_{c,χ_d} and the typical momentum $p_{c,\infty}$ (Eqs. 3.1-3.2). The UR (red) and NR (blue) limits are shown separately, with dashed lines indicating singularities.

that rather than being energized at the thermal energy scale, the typical particles are energized by an amount comparable to the free magnetic energy per particle, $E_{\rm free} = \delta B^2/8\pi n_0$, over a dynamical timescale, before equilibrating to the GME state. Here, δB is the characteristic magnetic field fluctuation, while we denote the background (non-dissipating) component by B_0. We denote the energy corresponding to the Casimir momenta by $E_{c,\chi} = E(p_{c,\chi})$ and the typical particle energy as E_0, noting that the thermal dissipation energy scale is eE_0. The model posits that $E_{c,\chi_d} \sim eE_0 + \eta E_{\rm free}$ where η is an order-unity coefficient describing the portion of free energy converted. We can then write

$$
\begin{aligned}
\frac{p_{c,\chi_d}}{p_{c,\infty}} &= \left[\frac{E_{c,\chi_d}(E_{c,\chi_d}+2mc^2)}{E_{c,\infty}(E_{c,\infty}+2mc^2)}\right]^{1/2} \\
&\sim \left[\frac{(eE_0+\eta E_{\rm free})(eE_0+\eta E_{\rm free}+2mc^2)}{E_0(E_0+2mc^2)}\right]^{1/2} \\
&\sim \left[\frac{[e+\eta(\delta B/B_0)^2/\beta_c][e+\eta(\delta B/B_0)^2/\beta_c+2/\theta_c]}{1+2/\theta_c}\right]^{1/2} ,
\end{aligned} \tag{3.3}
$$

where $\theta_c = E_0/mc^2$ is a characteristic dimensionless temperature and $\beta_c = 8\pi n_0 E_0/B_0^2$ is a characteristic plasma beta for the particle species (which may differ from the standard plasma beta, $\beta_0 = 8\pi n_0 T/B_0^2$ where T is species temperature, by a factor of order unity). Equating Eq. 3.3 with either Eq. 3.1 or Eq. 3.2 yields an implicit equation for α as a function of β_c, $\delta B/B_0$, and θ_c in the appropriate limit. The physical parameters required to achieve a given value of α can then be expressed in the UR limit ($\theta_c \gg 1$) as:

$$
\eta \left(\frac{\delta B}{B_0}\right)^2 \frac{1}{\beta_c} \stackrel{\rm UR}{=} \left(\frac{\alpha+1}{\alpha-2}\right)^{(\alpha+2)/3} - e\,, \tag{3.4}
$$

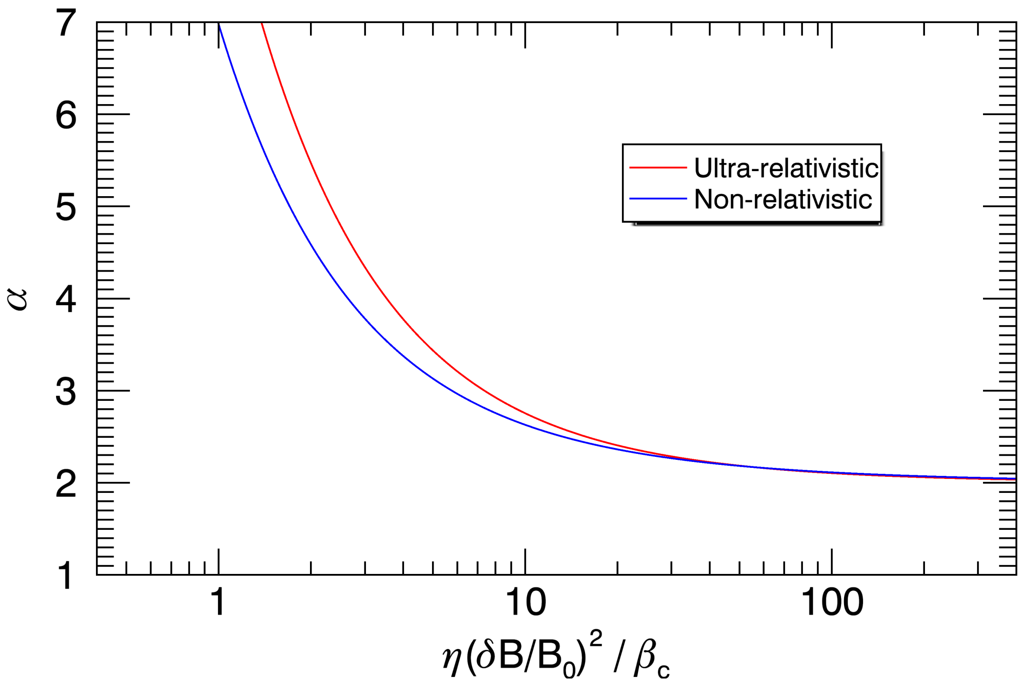

FIGURE 2. The energy power-law index α of the GME distribution versus physical parameters $\eta(\delta B/B_0)^2/\beta_c$ for the magnetic dissipation model. The UR (red; Eq. 3.4) and NR (blue; Eq. 3.5) limits are shown separately.

and in the NR limit ($\theta_c \ll 1$) as:

$$\eta \left(\frac{\delta B}{B_0}\right)^2 \frac{1}{\beta_c} \stackrel{\rm NR}{=} \left(\frac{\alpha - 1/2}{\alpha - 2}\right)^{(2\alpha+1)/3} - e\,. \tag{3.5}$$

The predicted scaling of α given by Eqs. 3.4-3.5 is the second main result of this work. The right hand side of both equations becomes zero when $\alpha \to \infty$, indicating that the thermal distribution is recovered for high beta or weak fluctuations, $(\delta B/B_0)^2/\beta_c \ll 1$. On the other hand, the nonthermal state is obtained when $(\delta B/B_0)^2/\beta_c \gtrsim 1$, for both UR and NR regimes. For $(\delta B/B_0)^2/\beta_c \gg 1$, $\alpha \to 2$. The scaling is plotted in Fig. 2.

4. Comparison to simulations

To validate the GME model, we remark on how the predictions compare to existing results from kinetic simulations of relativistic turbulence and magnetic reconnection in the literature.

In Fig. 3, we show the global particle energy distribution $F(E)$ arising in a 1536^3-cell particle-in-cell (PIC) simulation of driven relativistic turbulence (with $\delta B/B_0 \approx 1$) studied in Refs. (Zhdankin *et al.* 2018; Wong *et al.* 2020). The simulation begins with a Maxwell-Jüttner distribution of electrons and positrons with UR temperature $\theta = T/m_e c^2 = 100$ and initial magnetization $\sigma_0 = 3/8$. The magnetization is defined as the ratio of the magnetic enthalpy to plasma enthalpy, and is related to species plasma beta by $\sigma_0 = 1/(4\beta_0)$ in the UR regime; thus $\beta_0 = 2/3$. The simulation develops a nonthermal tail with index $\alpha \approx 3$. We find that the GME distribution of Eq. 2.5 provides a fair fit to the fully developed state when we choose $\chi_d = 0.815$, as shown by the dashed

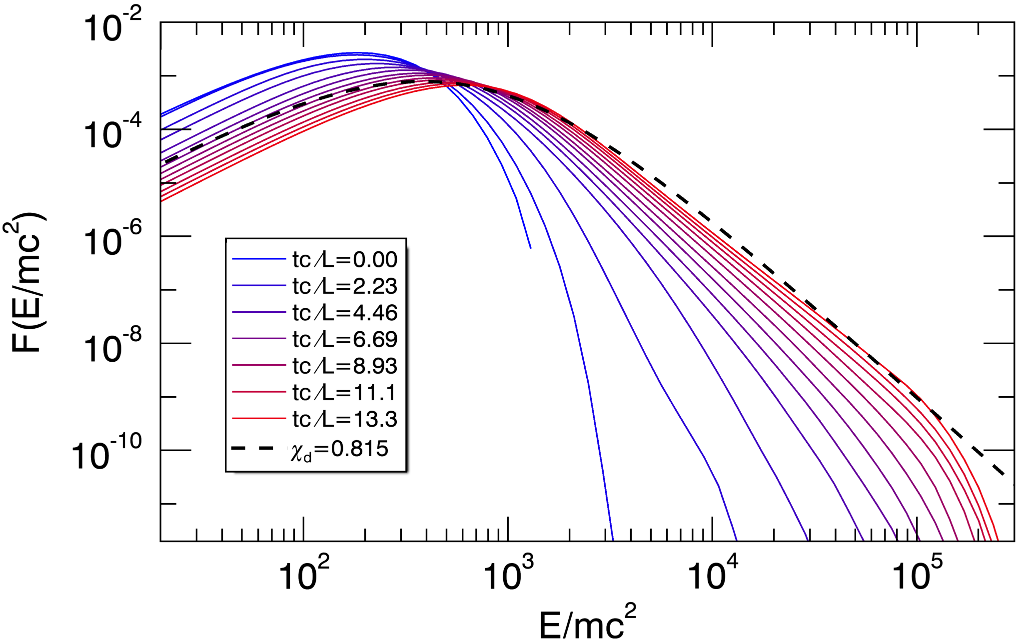

FIGURE 3. Energy distribution $F(E)$ in PIC simulation of relativistic turbulence for various times, compared to the GME distribution (dashed; Eq. 2.5) with $\chi_d = 0.815$.

line in Fig. 3. The fit over-predicts the number of particles at energies below the peak, indicating that relaxation to the GME state is incomplete (possible reasons for this will be described in the conclusions). The PIC simulations of decaying, magnetically-dominated turbulence by Comisso & Sironi (2019) also appear to resemble the GME state. Thus, we believe that the GME model provides a reasonable (if imperfect) representation of available numerical data on relativistic turbulence.

We next consider the model for the power-law index α from magnetic dissipation. In Fig. 4, we compare the predicted α versus σ scaling (Eq. 3.4 with $\beta_c = 1/4\sigma$, $\delta B/B_0 = 1$, $\eta = 1$) with results in the literature on relativistic turbulence in pair plasma. PIC simulations of driven relativistic turbulence indicate that the power-law index is well-described by the empirical formula $\alpha \approx \alpha_\infty + C_0\sigma^{-0.5}$, with $\alpha_\infty \approx 1$ and $C_0 \approx 1.5$ for large sizes (Zhdankin *et al.* 2017, 2018), shown in Fig. 4 (blue); note that a similar formula with different coefficients was also suggested for relativistic magnetic reconnection (Werner *et al.* 2018; Ball *et al.* 2018; Uzdensky 2022). We also show approximate data points from the 2D decaying relativistic turbulence simulations of Comisso & Sironi (2019) (red). The model is able to explain the trends in the numerical simulations fairly well, up to a factor of order unity in σ. Fits to the simulation data can be improved by adjusting η, noting that driven turbulence would effectively have a larger η than decaying turbulence. Additionally, we note that Comisso & Sironi (2019) finds that α increases with decreasing $\delta B/B_0$, consistent with the GME prediction.

In addition to these quantitative comparisons, the GME model provides a resolution to several mysterious findings from kinetic simulations in the literature. Kinetic simulations of disparate processes (turbulence, magnetic reconnection, and instabilities) often exhibit very similar power-law distributions for given plasma parameters. For example, PIC simulations find comparable nonthermal particle acceleration from magnetic dissipation with different current sheet geometries and ensuing dynamics (e.g., Werner & Uzdensky

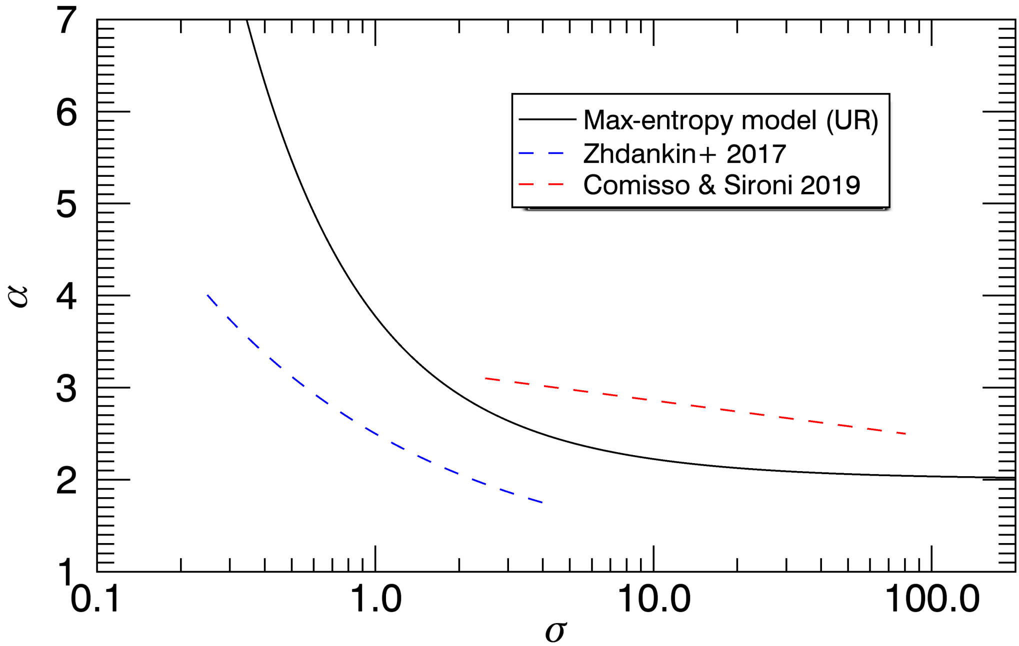

FIGURE 4. Energy power-law index α versus magnetization σ from the GME model in the UR limit (black; Eq. 3.4 with $\beta_c = 1/4\sigma$, $\delta B/B_0 = 1$, and $\eta = 1$) compared to empirical fitting formula $\alpha \approx \alpha_\infty + C_0\sigma^{-0.5}$ from PIC simulations of driven relativistic turbulence in Ref. (Zhdankin *et al.* 2017) (blue). Also shown is the approximate range of indices from PIC simulations of decaying relativistic turbulence from Ref. (Comisso & Sironi 2019) (their Fig. 5 inset; red).

2021). PIC simulations of relativistic turbulence find that nonthermal particle distributions have a similar shape for different driving mechanisms (electromagnetic, solenoidal, compressive, imbalanced), despite different timescales to arrive at those distributions (Zhdankin 2021; Hankla *et al.* 2022). The universality revealed by these findings may be explained by all of the processes having sufficient complexity to attain a GME state at similar energy scales.

Kinetic simulations also indicate that nonthermal particle distributions formed by relativistic magnetic reconnection (Werner & Uzdensky 2017; Guo *et al.* 2021) and turbulence (Comisso & Sironi 2019) are insensitive to the number of spatial dimensions (2D vs 3D), despite different secondary instabilities, cascades, and trapping mechanisms (e.g., long-lived plasmoids in 2D). The GME framework predicts that the distributions are insensitive to the number of spatial dimensions, as long as there are sufficient degrees of freedom to attain such a state.

The GME model predicts similar acceleration efficiency in the NR regime as in the UR regime. PIC simulations in the NR regime are generally constrained in scale separation, which may limit power-law formation. However, recent PIC simulations of NR magnetic reconnection provide some evidence for (steep) power-law distributions at low β (Li *et al.* 2019). Recent simulations of reduced kinetic models indicate efficient electron acceleration by NR magnetic reconnection at macroscopic scales when $\delta B/B_0$ is moderate (Arnold *et al.* 2021), lending support to the GME model. Further benchmarking of the model in the NR regime is deferred to future work.

5. Conclusions

This Letter provides an analytical model for power-law nonthermal distributions that arise in collisionless plasmas due to generic energization processes. Unlike many works in the literature, this model is based on maximum entropy principles (of a generalized, non-BG form), rather than the details of the microscopic mechanisms that ultimately enable (or counteract) the acceleration. The GME distribution (Eqs. 2.4-2.6) provides a physically-motivated reduced model for nonthermal particle populations. Likewise, the model for the power-law index α of the equilibrium distribution versus plasma parameters (Eqs. 3.4-3.5) may be a useful prescription for systems where magnetic dissipation is the key energizer (e.g., magnetic reconnection, turbulence, and some instabilities). Further comparison to kinetic simulations will be essential for benchmarking the validity of the model and determining a more rigorous closure for $p_{c,\chi_d}/p_{c,\infty}$.

There are several physical effects that may prevent the nonthermal GME state described in this Letter from being attained in some systems. First and foremost, the competition of entropy production mechanisms at multiple scales would invalidate the core assumption of the distribution being governed by $p_{c,\chi}$ at a single dominant value of the index $\chi = \chi_d$. Second, the time-dependence of physical parameters may cause $p_{c,\chi_d}/p_{c,\infty}$ to vary over time, leading to hysteresis that is not accounted for in the model. These assumptions may be relaxed in future iterations of the model.

Another effect that may prevent the GME state from being attained is anisotropy of the momentum distribution (at macroscopic scales). This may occur if the energization mechanisms are strongly anisotropic with respect to the large-scale magnetic field and pitch angle scattering is inefficient. Anisotropy reduces the entropy and thus prevents complete relaxation to the (isotropic) GME state.

The GME model indicates that particle acceleration will be inefficient if the mechanisms of entropy production are localized at energy scales near the thermal energy (Landau damping being one such example). This may be the situation for simplified or dynamically constrained setups such as the collision of Alfvén waves (Nättilä & Beloborodov 2022), 2D NR magnetic reconnection (Dahlin *et al.* 2017; Li *et al.* 2019), or magnetic reconnection in a strong guide field (Werner & Uzdensky 2017; Arnold *et al.* 2021).

Nonthermal particle acceleration is usually modeled in the language of quasilinear theory, involving concepts such as the Fokker-Planck equation (or its extensions), pitch-angle scattering, and trapping (or escape) mechanisms (see, e.g., Kulsrud & Ferrari 1971; Blandford & Eichler 1987; Schlickeiser 1989; Chandran 2000; Isliker *et al.* 2017; Lemoine & Malkov 2020; Demidem *et al.* 2020; Lemoine 2021; Vega *et al.* 2022). The maximum-entropy model proposed in this Letter stands in stark contrast to these conventional approaches, being only weakly dependent on the physical ingredients responsible for enabling the GME state. The two frameworks are not mutually exclusive, however, as the GME distribution may be maintained by a broad class of Fokker-Planck diffusion/advection coefficients (e.g., Shizgal 2018). It is important for future work to bridge the two mathematical frameworks.

The author thanks Dmitri Uzdensky, Mitch Begelman, Greg Werner, and Yuri Levin for helpful discussions during the early stages of this project. Research at the Flatiron Institute is supported by the Simons Foundation.

REFERENCES

Alves, E. P., Zrake, J. & Fiuza, F. 2018 Efficient nonthermal particle acceleration by the kink instability in relativistic jets. *Physical review letters* **121** (24), 245101.

Arnold, H., Drake, J., Swisdak, M., Guo, F., Dahlin, J., Chen, B., Fleishman, G., Glesener, L., Kontar, E., Phan, T. & others 2021 Electron acceleration during macroscale magnetic reconnection. *Physical review letters* **126** (13), 135101.

Aschwanden, M. J. 2002 Particle acceleration and kinematics in solar flares–a synthesis of recent observations and theoretical concepts (invited review). *Space Science Reviews* **101** (1-2), 1–227.

Ball, D., Sironi, L. & Özel, F. 2018 Electron and proton acceleration in trans-relativistic magnetic reconnection: dependence on plasma beta and magnetization. *The Astrophysical Journal* **862** (1), 80.

Birn, J., Artemyev, A., Baker, D., Echim, M., Hoshino, M. & Zelenyi, L. 2012 Particle acceleration in the magnetotail and aurora. *Space science reviews* **173** (1-4), 49–102.

Blandford, R. & Eichler, D. 1987 Particle acceleration at astrophysical shocks: A theory of cosmic ray origin. *Physics Reports* **154** (1), 1–75.

Caprioli, D. & Spitkovsky, A. 2014 Simulations of ion acceleration at non-relativistic shocks. i. acceleration efficiency. *The Astrophysical Journal* **783** (2), 91.

Chandran, B. D. 2000 Scattering of energetic particles by anisotropic magnetohydrodynamic turbulence with a goldreich-sridhar power spectrum. *Physical Review Letters* **85** (22), 4656.

Comisso, L. & Sironi, L. 2018 Particle acceleration in relativistic plasma turbulence. *Physical review letters* **121** (25), 255101.

Comisso, L. & Sironi, L. 2019 The interplay of magnetically dominated turbulence and magnetic reconnection in producing nonthermal particles. *The Astrophysical Journal* **886** (2), 122.

Dahlin, J., Drake, J. & Swisdak, M. 2017 The role of three-dimensional transport in driving enhanced electron acceleration during magnetic reconnection. *Physics of Plasmas* **24** (9), 092110.

Demidem, C., Lemoine, M. & Casse, F. 2020 Particle acceleration in relativistic turbulence: A theoretical appraisal. *Physical Review D* **102** (2), 023003.

Eyink, G. L. 2018 Cascades and dissipative anomalies in nearly collisionless plasma turbulence. *Physical Review X* **8** (4), 041020.

Fermi, E. 1949 On the origin of the cosmic radiation. *Physical Review* **75** (8), 1169.

Fermi, E. 1954 Galactic magnetic fields and the origin of cosmic radiation. *The Astrophysical Journal* **119**, 1.

Fisk, L. & Gloeckler, G. 2007 Acceleration and composition of solar wind suprathermal tails. *Space science reviews* **130** (1-4), 153–160.

Guo, F., Li, H., Daughton, W. & Liu, Y.-H. 2014 Formation of hard power laws in the energetic particle spectra resulting from relativistic magnetic reconnection. *Physical Review Letters* **113**, 155005.

Guo, F., Li, X., Daughton, W., Li, H., Kilian, P., Liu, Y.-H., Zhang, Q. & Zhang, H. 2021 Magnetic energy release, plasma dynamics, and particle acceleration in relativistic turbulent magnetic reconnection. *The Astrophysical Journal* **919** (2), 111.

Hankla, A. M., Zhdankin, V., Werner, G. R., Uzdensky, D. A. & Begelman, M. C. 2022 Kinetic simulations of imbalanced turbulence in a relativistic plasma: Net flow and particle acceleration. *Monthly Notices of the Royal Astronomical Society* **509** (3), 3826–3841.

Hoshino, M. 2013 Particle acceleration during magnetorotational instability in a collisionless accretion disk. *The Astrophysical Journal* **773** (2), 118.

Isliker, H., Vlahos, L. & Constantinescu, D. 2017 Fractional transport in strongly turbulent plasmas. *Physical Review Letters* **119** (4), 045101.

Kulsrud, R. M. & Ferrari, A. 1971 The relativistic quasilinear theory of particle acceleration by hydromagnetic turbulence. *Astrophysics and Space Science* **12** (2), 302–318.

Kunz, M. W., Stone, J. M. & Quataert, E. 2016 Magnetorotational turbulence and dynamo in a collisionless plasma. *Physical Review Letters* **117** (23), 235101.

Lemoine, M. 2021 Particle acceleration in strong mhd turbulence. *Physical Review D* **104** (6), 063020.

Lemoine, M. & Malkov, M. A. 2020 Power-law spectra from stochastic acceleration. *Monthly Notices of the Royal Astronomical Society* **499** (4), 4972–4983.

Leubner, M. P. 2002 A nonextensive entropy approach to kappa-distributions. *Astrophysics and space science* **282** (3), 573–579.

Ley, F., Riquelme, M., Sironi, L., Verscharen, D. & Sandoval, A. 2019 Stochastic ion acceleration by the ion-cyclotron instability in a growing magnetic field. *The Astrophysical Journal* **880** (2), 100.

Li, X., Guo, F., Li, H., Stanier, A. & Kilian, P. 2019 Formation of power-law electron energy spectra in three-dimensional low-β magnetic reconnection. *The Astrophysical Journal* **884** (2), 118.

Livadiotis, G. & McComas, D. 2009 Beyond kappa distributions: Exploiting tsallis statistical mechanics in space plasmas. *Journal of Geophysical Research: Space Physics* **114** (A11).

Livadiotis, G. & McComas, D. 2013 Understanding kappa distributions: A toolbox for space science and astrophysics. *Space Science Reviews* **175** (1), 183–214.

Milovanov, A. & Zelenyi, L. 2000 Functional background of the tsallis entropy:" coarse-grained" systems and" kappa" distribution functions. *Nonlinear Processes in Geophysics* **7** (3/4), 211–221.

Nalewajko, K., Zrake, J., Yuan, Y., East, W. E. & Blandford, R. D. 2016 Kinetic Simulations of the Lowest-order Unstable Mode of Relativistic Magnetostatic Equilibria. *The Astrophysical Journal* **826**, 115.

Nättilä, J. & Beloborodov, A. M. 2022 Heating of magnetically dominated plasma by alfvén-wave turbulence. *Physical Review Letters* **128** (7), 075101.

Parker, E. & Tidman, D. 1958 Suprathermal particles. *Physical Review* **111** (5), 1206.

Pierrard, V. & Lazar, M. 2010 Kappa distributions: theory and applications in space plasmas. *Solar physics* **267** (1), 153–174.

Rényi, A. 1961 On measures of entropy and information. In *Proceedings of the Fourth Berkeley Symposium on Mathematical Statistics and Probability, Volume 1: Contributions to the Theory of Statistics*, pp. 547–561. University of California Press.

Schekochihin, A., Cowley, S., Dorland, W., Hammett, G., Howes, G., Quataert, E. & Tatsuno, T. 2009 Astrophysical gyrokinetics: kinetic and fluid turbulent cascades in magnetized weakly collisional plasmas. *The Astrophysical Journal Supplement Series* **182** (1), 310.

Schlickeiser, R. 1989 Cosmic-ray transport and acceleration. i-derivation of the kinetic equation and application to cosmic rays in static cold media. ii-cosmic rays in moving cold media with application to diffusive shock wave acceleration. *The Astrophysical Journal* **336**, 243–293.

Shizgal, B. D. 2018 Kappa and other nonequilibrium distributions from the fokker-planck equation and the relationship to tsallis entropy. *Physical Review E* **97** (5), 052144.

Sironi, L., Rowan, M. E. & Narayan, R. 2021 Reconnection-driven particle acceleration in relativistic shear flows. *The Astrophysical Journal Letters* **907** (2), L44.

Sironi, L. & Spitkovsky, A. 2010 Particle acceleration in relativistic magnetized collisionless electron-ion shocks. *The Astrophysical Journal* **726** (2), 75.

Sironi, L. & Spitkovsky, A. 2014 Relativistic reconnection: an efficient source of non-thermal particles. *The Astrophysical Journal Letters* **783** (1), L21.

Spitkovsky, A. 2008 Particle acceleration in relativistic collisionless shocks: Fermi process at last? *The Astrophysical Journal Letters* **682** (1), L5.

Tsallis, C. 1988 Possible generalization of boltzmann-gibbs statistics. *Journal of statistical physics* **52** (1), 479–487.

Uzdensky, D. A. 2022 Relativistic non-thermal particle acceleration in two-dimensional collisionless magnetic reconnection. *Journal of Plasma Physics* **88** (1).

Vega, C., Boldyrev, S., Roytershteyn, V. & Medvedev, M. 2022 Turbulence and particle acceleration in a relativistic plasma. *The Astrophysical Journal Letters* **924** (1), L19.

Werner, G. R. & Uzdensky, D. A. 2017 Nonthermal particle acceleration in 3d relativistic magnetic reconnection in pair plasma. *The Astrophysical Journal Letters* **843** (2), L27.

Werner, G. R. & Uzdensky, D. A. 2021 Reconnection and particle acceleration in three-dimensional current sheet evolution in moderately magnetized astrophysical pair plasma. *Journal of Plasma Physics* **87** (6).

Werner, G. R., Uzdensky, D. A., Begelman, M. C., Cerutti, B. & Nalewajko, K. 2018

Non-thermal particle acceleration in collisionless relativistic electron-proton reconnection. *Monthly Notices of the Royal Astronomical Society* **473**, 4840–4861.

Werner, G. R., Uzdensky, D. A., Cerutti, B., Nalewajko, K. & Begelman, M. C. 2016 The Extent of Power-law Energy Spectra in Collisionless Relativistic Magnetic Reconnection in Pair Plasmas. *The Astrophysical Journal Letters* **816**, L8.

Wong, K., Zhdankin, V., Uzdensky, D. A., Werner, G. R. & Begelman, M. C. 2020 First-principles demonstration of diffusive-advective particle acceleration in kinetic simulations of relativistic plasma turbulence. *The Astrophysical Journal Letters* **893** (1), L7.

Zhdankin, V. 2021 Generalized entropy production in collisionless plasma flows and turbulence. *arXiv preprint arXiv:2110.07025* .

Zhdankin, V. 2021 Particle Energization in Relativistic Plasma Turbulence: Solenoidal versus Compressive Driving. *The Astrophysical Journal* **922** (2), 172.

Zhdankin, V., Uzdensky, D. A., Werner, G. R. & Begelman, M. C. 2018 System-size convergence of nonthermal particle acceleration in relativistic plasma turbulence. *The Astrophysical Journal Letters* **867** (1), L18.

Zhdankin, V., Werner, G. R., Uzdensky, D. A. & Begelman, M. C. 2017 Kinetic turbulence in relativistic plasma: From thermal bath to nonthermal continuum. *Phys. Rev. Lett.* **118**, 055103.